Grazing Incidence X-ray Scattering and Diffraction

Jaydeep K Basu

Jaydeep K Basu is at the Physics department of the Indian Institute of Science, Bangalore. His area of current interest includes soft condensed matter Physics as well as nanophotonics and plasmonics. He uses both laboratory and synchrotron X-ray scattering based techniques for his research in soft matter Physics.

The advent of dedicated powerful synchrotron X-ray sources worldwide has lead to the growth of the most recent branch of X-ray diffraction and scattering – surface X-ray scattering and diffraction. In thia article, various aspects of surface X-ray diffraction and scattering are discussed with illustrations of some typical applications of these techniques.

1. Introduction

Have you ever wondered what makes diamonds glitter? Or have you pondered as to why the fingerprints of your hand holding a glass of water become visible? The next time you take a dip in a swimming pool, try watching the water surface from below while staying still – what do you see? Your own reflection! All these and several other more practical applications utilise the phenomenon of total internal reflection of ordinary light, i.e., electromagnetic (EM) radiation in the visible region. Total internal reflection (TIR) of light takes place only when light traveling in an optically denser medium (i.e., a medium with higher refractive index), is incident at its interface with a medium of lower refractive index is provided that the angle of incidence is equal to or larger than the critical angle for total internal reflection between the two media. The magnitude of the critical angle depends on the relative difference of refractive indices between the two media. Since light is an EM wave the phenomenon of total internal reflection can be understood in terms of the wave properties of EM radiation. So, do EM waves of all wavelengths exhibit only total internal reflection? The answer is NO! X-rays (as well as thermal neutrons) undergo what is called total

Keywords
X-ray reflectivity, X-ray diffuse scattering, grazing incident diffraction, grazing incident, small angle X-ray scattering.

external reflection (TER) at an interface! So is there a fundamental difference between ordinary light and X-rays?

X-rays propagate as evanescent waves within a small depth into a material medium.

To understand this, one needs to look at the mathematical expression for refractive index or more precisely the frequency dependence of the dielectric function of any material. Usually this is a complex function and is represented in terms of a sum of Lorentzian functions corresponding to certain transition frequencies. For most materials, these frequencies are in the UV–visible or lower frequency regions, hence, the dielectric constant or refractive index in the visible regime of the EM spectrum is greater than that of air/vacuum. However, at a very high frequency regime (like X-rays) it turns out that the refractive index for all materials is less than 1! The difference is extremely small but the refractive index is always smaller than 1. This implies that for X-rays we expect TER instead of TIR, since air is the medium with the highest refractive index as compared to any material medium for EM radiation at energies comparable to energy of X-rays (a few KeV). The value of a typical critical angle at the air–material interface is typically a few 100 milli degrees or less and depends on the energy of the incident X-rays as well as the electron density of the material. Thus, X-rays incident at angles smaller than or equal to the critical angle for the material, from air, will undergo TER and will not penetrate the bulk of the medium. More specifically, the X-rays propagate as evanescent waves within a small depth (typically a few nanometres) into the material medium. *Figure* 1 illustrates the variation of the penetration depth, μ for several materials as a function of angle of incidence, α_i with X-rays of wavelength 1.54 Å.

The advent of synchrotron radiation sources worldwide gave birth to the field of surface X-ray (and neutron) scattering and diffraction as a collection of techniques which enables structural studies of purely 2D materials

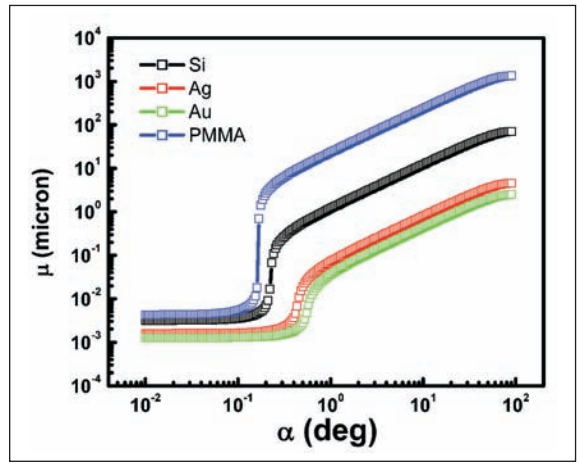

Figure 1. Penetration depth vs angle of incidence for an incident X-ray of wavelength 1.54Å of Silicon (Si), Silver (Ag), Gold (Au) and Poly(methyl methacrylate) (PMMA) with respect to air/ vacuum.

or studies of the surface of a bulk material or the interface between two bulk media. The main techniques which come under the ambit of grazing incidence X-ray scattering (GIXS) are: (i) X-ray reflectivity (XR); (ii) X-ray diffuse scattering (XDS); and (iii) grazing incidence small angle X-ray scattering (GISAXS). In this article, we will not discuss the related technique of SAXS which has been nicely covered in an earlier issue of *Resonance* by Raghunathan [1]. In addition, one can also perform diffraction measurements in what is called a grazing incidence diffraction (GID) geometry. *Figure* 2 explains the beam path and configuration for all the above mentioned modes of surface X-ray scattering and diffraction.

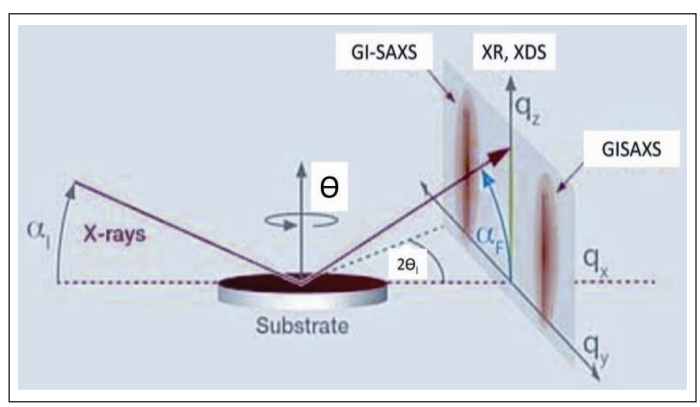

Figure 2. Schematic of XR, XDS and GISAXS.
(Adapted from www.saxspace.com)

We will first discuss the technique of X-ray reflectivity.

2. X-ray Reflectivity

It is possible to arrive at the basic expression for X-ray specular reflectivity of a smooth surface by solving the Maxwell's wave equations for scattering of electromagnetic waves at the surface under appropriate boundary conditions for the continuity of the electric field and its derivative. The refractive index n, of a homogeneous medium, with multiple species, can be written as

$$n = 1 - \delta + i\beta\,. \tag{1}$$

For X-rays, δ is given by

$$\delta = \frac{r_0\lambda^2}{2\pi} N_{\mathrm{A}} \sum_i \frac{\rho_i (Z_i + f_i')}{A_i} = \frac{r_0\lambda^2}{2\pi} \sum_i N_i = \frac{\lambda^2}{2\pi} \sum_i \varrho_i \tag{2}$$

and β is related to the imaginary anomalous dispersion factor f'' (which is related to the X-ray absorption coefficient) and can be written as

$$\beta = \frac{r_0\lambda^2}{2\pi} N_{\mathrm{A}} \sum_i \frac{\rho_i f_i''}{A_i}\ . \tag{3}$$

In the above expressions, r_0 is the classical electron radius given by e^2/mc^2 (which is equal to 2.8210^{-13} cm), Z_i and N_i are respectively the atomic number and electron number density of the i-th element and f' is the real anomalous dispersion factor. In vacuum, the z-component of the wave vector (normal to the surface or xy-plane) is given by

$$K_z = \frac{q_z}{2} = \frac{\pi(\sin\alpha_i + \sin\alpha_f)}{\lambda}\,, \tag{4}$$

where α_i is the grazing angle of incidence. In the specular condition, where the angle of incidence α_i is equal to the angle of reflection α_f, this is the same as the total wave vector K. At an interface separating two media

Under small angle approximation the critical wave vector is independent of the wavelength of X-ray and dependent only on the electron density of the material.

with refractive indices n_1 and n_2, the direction of the refracted beam can be obtained from Snell's law as

$$n_1 \cos\alpha_i = n_2 \cos\alpha_i'. \tag{5}$$

For the substrate with $n_1 = 1$ and $n_2 = n_0$, we can obtain a real angle of incidence for which the angle of refraction α_i' becomes zero provided $n_2 < n_1$ (which is the case for any material having finite electron density) and the corresponding grazing incident angle, known as the critical angle, α_c, can be written as

$$\cos\alpha_c = n_0 \,. \tag{6}$$

In the *small angle approximation*, the critical angle can be written as

$$\alpha_c = \sqrt{2\delta} = \sqrt{\frac{\lambda^2 N_A \rho r_0}{\pi A}} \,. \tag{7}$$

where δ is given by (2). Using the definition of refractive index $n_0 = K_{2z}/K_z$, we can get the expression (which is in general complex) for the z-component of the wave vector in the medium,

$$K_{2z} = [K^2 - K_c^2]^{1/2} \,, \tag{8}$$

where K_c is the critical wave vector given by

$$K_c = \frac{q_c}{2} = \frac{2\pi \sin\alpha_c}{\lambda} \,. \tag{9}$$

Again using small angle approximation, for a medium with $n_0 < 1$, we can calculate K_c and rewrite (8) as

$$K_{2z} = [K_z^2 - 4\pi N_A \rho r_0 / A]^{1/2} \,. \tag{10}$$

It is interesting to note that under small angle approximation, K_c is independent of wavelength in the X-ray energy range, and depends only on the electron density

of the material. The reflectance, r_{12}, for the substrate can then be written as

$$r_{12} = \frac{K_z - K_{2z}}{K_z + K_{2z}} = \frac{q_z - q_{2z}}{q_z + q_{2z}}. \tag{11}$$

The specular reflectivity $R = r_{12}r_{12}^*$ can then be written in two equivalent forms as

$$R = \left| \frac{\sin\alpha_i - n_0 \sin\alpha_i'}{\sin\alpha_i + n_0 \sin\alpha_i'} \right|^2, \tag{12}$$

$$R = \left| \frac{K_z - \sqrt{K_z^2 - K_c^2}}{K_z + \sqrt{K_z^2 - K_c^2}} \right|^2. \tag{13}$$

The above expressions are known as the Fresnel law of reflectivity.

2.1 *Reflectivity from Multiple Interfaces*

In the case of a thin film of finite thickness d, we have to solve the wave equations at two interfaces, namely film–vacuum/air (at $z = 0$) and substrate–film (at $z = d$). It is interesting to note that the continuity condition at $z = d$ will generate an extra factor, which in turn will give the reflectance at the film–substrate interface as

$$r_{23} = \frac{K_{2z} - K_{3z}}{K_{2z} + K_{3z}} \exp(-2iK_{2z}d)\,. \tag{14}$$

Using simple algebra and noting the fact that $r_{21} = r_{12}$, we can write the reflectance from this thin film substrate system as

$$r_0 = \frac{r_{12} + r_{23}}{1 + r_{12}r_{23}}\,. \tag{15}$$

We can easily extend the above calculation to the case of reflectivity for a system having M such thin layers (stratified homogeneous media), having smooth interfaces. We denote the thickness of each layer by d_n. A set

of simultaneous equations similar to (15) can be solved and one can arrive at a recursive formula given by

$$r_{n-1,n} = \exp(-2iK_{(n-1)z}d_{n-1})\frac{r_{n,n+1} + F_{n-1,n}}{1 + r_{n,n+1}F_{n-1,n}}, \quad (16)$$

where

$$F_{n-1,n} = \frac{K_{(n-1)z} - K_{nz}}{K_{(n-1)z} + K_{nz}}. \quad (17)$$

To obtain the reflectivity of this system, one solves the recursive relation given by (16) from the bottom layer with the knowledge that $r_{n,n+1} = 0$, since the thickness of this medium (normally the substrate) can be taken as infinite.

The reflectivity of a rough surface is smaller than the reflectivity of a smooth surface and this deviation increases with q_z.

So far, we have dealt only with smooth surfaces and interfaces. At this stage, we can introduce the concept of roughness. It is known that the reflectivity of a rough surface is smaller than the reflectivity of a smooth surface and this deviation increases with q_z. One can calculate the effect of roughness by approximating the scattering density profile with a series of discrete layers as discussed above and using the iterative scheme of (16). Actually, the first derivative of the scattering profile can be described, for most of the cases, as a Gaussian function. Therefore, by using Born approximation, one can write the reflectance of a rough surface as

$$r_{n-1,n} = r^F_{n-1,n}\exp(-0.5q_{(n-1)z}q_{nz}\sigma_n^2). \quad (18)$$

The parameter σ_n is the measure of roughness between (n–1)th and nth interfaces, and roughness acts like a Debye Waller Factor[1]. Equation (18) also explains the observation that reflectance of rough surface ($r_{n-1,n}$) deviates more from the reflectance for smooth surface, $r^F_{n-1,n}$ as $q_{(n-1)z}$ and q_{nz} increase with q_z. For a surface separating two media 1 and 2, (18) can be simplified, to obtain the reflectivity as

$$R_{\text{rough}} = R_{\text{F}}\exp(-q_z^2\sigma_{12}^2), \quad (19)$$

[1] The Debye–Waller factor (DWF), named after Peter Debye and Ivar Waller, is used in condensed matter physics to describe the attenuation of x-ray scattering or coherent neutron scattering caused by thermal motion.

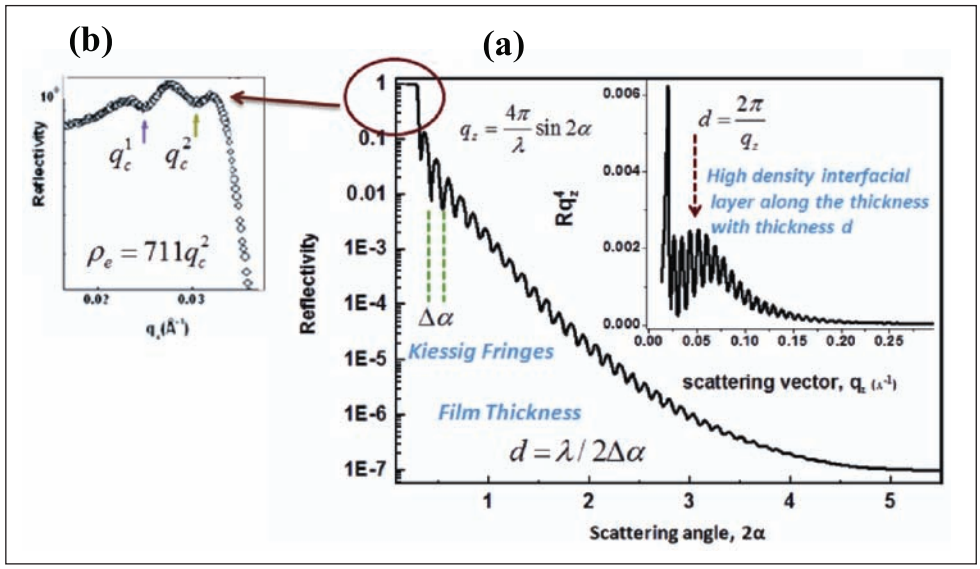

Figure 3. a) Reflectivity vs scattering angle showing the relation of film thickness with the period of fringes. Inset shows normalized reflectivity profile, R vs q_z^4 (b) Zoomed in region of reflectivity highlighting the importance of critical angle.
(Adapted from Sivasurender Chandran, Nafisa Begam and J K Basu *JAP*, 2014)

where R_F is the Fresnel reflectivity given in (12) and (13), and σ_{12} represents the roughness between the interface separating media 1 and 2. In general, the roughness of the film surface brings down the reflectivity curve faster; on the other hand, the roughness of the interface of the film and the substrate reduces the amplitudes of multilayer peaks. *Figure* 3 shows typical specular reflectivity data from a film on a substrate multilayer film on a substrate. The critical angles visible in *Figure* 3b correspond to, respectively, the different layers of the film and the substrate.

2. X-ray Diffuse Scattering

In the previous section, we discussed the basic formalism for X-ray reflectivity from smooth surfaces and interfaces. Although we did discuss rough surfaces, the effect of roughness was introduced by using the Born approximation. Moreover, our discussion was restricted to specular reflectivity, even for the rough surfaces. A large body of work exists on the scattering of electromagnetic radiation (mostly light or radio waves) from rough surfaces. In this regime, the interaction of the electromagnetic waves with matter is quite strong, and

the relevant wave equations are quite difficult to solve as they involve matching of boundary conditions over random rough surfaces. X-rays and neutrons, on the other hand, interact quite weakly with matter and hence, the solution of the wave equations can be performed under Born approximation.

For a plane wave incident on a medium with scattering length[2] density ρ, the solution of the wave equation can be written in general as

$$\psi(r) = e^{ik_i.r} + \frac{e^{ikr}}{r} f(k_f, k_i)\,, \tag{20}$$

where the scattering amplitude, $f(k_f, k_i)$, is given by

$$f(k_f, k_i) = \int \mathrm{d}r' \rho(r') \psi(r') e^{ik_f.r'}\,, \tag{21}$$

with k_i, k_f being the incident and scattered wave vectors, respectively. The above expression for scattering amplitude includes multiple scattering effects. If the interaction between the incident plane wave and the medium is sufficiently weak, then the first Born approximation, can be applied. In this approximation, the scattered wave function $\psi(r')$ can be assumed to be the same as the incident plane wave and hence the scattering amplitude takes a simpler form

$$f(k_f, k_i) = \int \mathrm{d}r' \varrho(r') e^{iq.r'}\,, \tag{22}$$

where $q = k_f - k_i$. The quantity that is measured experimentally is not the scattering amplitude but the differential scattering cross-section defined as

$$\frac{\mathrm{d}\sigma}{\mathrm{d}\Omega} = |f(k_f, k_i)|^2\,. \tag{23}$$

For a typical rough surface and applying (22) and (23), one can write

$$\frac{\mathrm{d}\sigma}{\mathrm{d}\Omega} = \rho^2 r_0^2 \left| \int_{-\infty}^{z(x,y)} \mathrm{d}z e^{-iq_z z} \int_{-\infty}^{+\infty} \mathrm{d}x \mathrm{d}y e^{-iq_x x} e^{-iq_y y} \right|^2 . \tag{24}$$

[2] Total scattered beam can be assumed as the scattered flux received by a surface of area, σ which is placed perpendicular to the incident beam. This area σ is called total scattering cross-section. This surface area can be related to a parameter which has a dimension of length, b, as $\sigma = 4\pi b^2$. Here, b is defined as the scattering length. For further reading refer to David J Griffiths, *Introduction to Quantum Mechanics*, Prentice Hall, 1994.

Here, $\varrho = \rho r_0$, with ρ being the electron density in the case of X-rays and r_0 the scattering length (or classical radius) of electrons. For neutrons, the corresponding quantities are the number density and the neutron scattering length b, respectively. The above equation can be further simplified to

$$\frac{\mathrm{d}\sigma}{\mathrm{d}\Omega} = \frac{\rho^2 r_0^2}{q_z^2} \int_{-\infty}^{\infty} \mathrm{d}x\mathrm{d}y \int_{-\infty}^{\infty} \mathrm{d}x'\mathrm{d}y' \exp(-q_z[z(x,y) - z(x',y')]) \times \exp(-[q_x(x-x') + q_y(y-y')]). \quad (25)$$

To proceed further, we need to formulate a geometrical description of a rough surface. It has been found that this can be done conveniently using the concept of fractals. Let us assume that $U = z(x,y) - z(x',y')$ is a *Gaussian random variable* whose probability distribution depends on the relative coordinates $(X,Y) = (x-x', y-y')$. Using this variable, one can define a quantity called the height difference correlation function $g(X,Y)$ as,

$$g(X,Y) = \langle [z(x',y') - z(x,y)]^2 \rangle \ , \quad (26)$$

where the average denotes an ensemble average over all possible configurations of the surface. Here, an implicit assumption has been made about the *stationarity* and *ergodicity* of the *Gaussian random variable* U. There are several advantages of using this formulation for the description of surface morphology. For random variables U, $\langle U^2 \rangle = \langle U \rangle^2 + \sigma^2$, where $\sigma = \sqrt{\langle U - \langle U \rangle \rangle^2}$. For the rough surface, the heights are defined with respect to a reference surface $\langle U \rangle = 0$. Hence, in this case $\langle U^2 \rangle = \sigma^2$. In the context of description of surface morphology, σ^2 is defined as the rms roughness of the surface. For a commonly observed type of rough surface, the rms roughness scales as a self-affine fractal[3]. Since statistically $g(X,Y)$ is equivalent to σ^2, for isotropic self-affine rough surfaces $g(X,Y)$ can be written as

$$g(X,Y) = g(r) = Ar^{2\gamma}, \ (0 < \gamma < 1) \ , \quad (27)$$

[3] A fractal is a natural phenomenon or a mathematical set that exhibits a repeating pattern that displays at every scale. If the replication is exactly the same at every scale, it is called a self-similar pattern. Self-affinity refers to a fractal whose pieces are scaled by different amounts in the *x*- and *y*-directions. For further details refer to Benoît B Mandelbrot, *The Fractal Geometry of Nature*, Macmillan, 1983.

where $r = \sqrt{X^2 + Y^2}$. This is, of course, an ideal description of a surface since for most surfaces in Nature $g(r)$ scales as a self-affine fractal only within a finite length scale, usually limited by system size. Using the definition of $g(X, Y) = g(r)$ in (26) we can write

$$g(r) = \langle z(0)\rangle^2 + \langle z(r)\rangle^2 - 2\langle z(0)z(r)\rangle = 2\sigma^2 - 2C(r). \tag{28}$$

Here $\langle z(0)\rangle^2 = \langle z(r)\rangle^2 = \sigma^2$. This is valid only under the assumption of *stationarity* of U. $C(r) = \langle z(0)z(r)\rangle$ is defined as the 'height–height' correlation of the surface. It can have different forms but the form that is used most commonly is

$$C(r) = \sigma^2 \exp(-r/\xi)^{2\gamma}\,. \tag{29}$$

Here, ξ is the cutoff length for height–height correlation of the surface. Using the above definitions, $g(r)$ for isotropic rough surfaces with cutoff can be written as

$$g(r) = 2\sigma^2[1 - \exp(-r/\xi)^{2\gamma}]\,. \tag{30}$$

Having developed the formalism for the statistical description of rough surfaces, we can now write down the expression for the structure factor and hence, intensity of the scattered beam from a rough surface, under the Born approximation, using the variables defined above. To calculate the scattering cross-section, a configurational average has to be performed over the different possible configurations of the random rough surface. Thus $\mathrm{d}\sigma/\mathrm{d}\Omega$ becomes

$$\frac{\mathrm{d}\sigma}{\mathrm{d}\Omega} = \frac{\rho^2 r_0^2}{q_z^2} \int_{-\infty}^{\infty} \mathrm{d}x\mathrm{d}y \int_{-\infty}^{\infty} \mathrm{d}x'\mathrm{d}y' \exp(-\langle q_z[z(x,y) - z(x',y')]\rangle) \exp(-[q_x(x-x') + q_y(y-y')])\,. \tag{31}$$

For Gaussian random variable,

$$\langle \exp(-iq_z[z(x,y) - z(x',y')])\rangle = \exp\left(-\tfrac{1}{2}q_z^2\langle[z(x,y) - z(x',y')]\rangle^2\right). \tag{32}$$

Hence, with the appropriate change of variables, we can write

$$\frac{\mathrm{d}\sigma}{\mathrm{d}\Omega} = \frac{\rho^2 r_0^2}{q_z^2} A \int_{-\infty}^{\infty} \mathrm{d}X \mathrm{d}Y e^{-q_z^2 g(X,Y)/2} e^{-i(q_x X + q_y Y)}. \quad (33)$$

Here, A is the area of the surface illuminated by the incident beam. The actual intensity detected in an experiment is obtained by convolution of the appropriate instrumental resolution function with the calculated scattering cross-section.

We next show how it is possible to arrive at the expression for specular reflectivity for a single smooth surface from (33), under the Born approximation. For a smooth surface, $g(r) = 0$. Hence, putting $g(r) = 0$ in (33), we get

$$\frac{\mathrm{d}\sigma}{\mathrm{d}\Omega} = 4\pi^2 \frac{\rho^2 r_0^2}{q_z^2} A \delta(q_x)\delta(q_y)\,, \quad (34)$$

where

$$\delta(q_x) = \frac{1}{2\pi} \int_{-\infty}^{\infty} \mathrm{d}X e^{-iq_x X}. \quad (35)$$

Reflectivity is defined as $R = I^{\mathrm{det}}/I^{\mathrm{inc}}$, where I^{det} is the intensity received by the detector and I^{inc}, the incident beam intensity, is given by incident beam flux $\times$ area of the beam normal to the surface which is $A\mathrm{sin}\alpha_i$. Hence, we can write reflectivity R as

$$R = \frac{1}{A\mathrm{sin}\alpha_i} \int \frac{\mathrm{d}\sigma}{\mathrm{d}\Omega} \mathrm{d}\Omega = \frac{4\pi^2}{q_z^2} \rho^2 r_0^2 \frac{1}{\mathrm{sin}\alpha_i} \int \delta(q_x)\delta(q_y)\mathrm{d}\Omega\,. \quad (36)$$

Using transformation of coordinates, $\mathrm{d}\Omega$ can be written as

$$\mathrm{d}\Omega = \frac{\mathrm{d}q_x \mathrm{d}q_y}{k_0^2\,\mathrm{sin}\alpha_i}. \quad (37)$$

Using (37) in (36), reflectivity R can be written as

$$R = \frac{16\pi^2 \rho^2 r_0^2}{q_z^4}. \quad (38)$$

This expression is the Fresnel reflectivity of a smooth surface under the Born approximation and can be obtained in the asymptotic limit of the exact Fresnel reflectivity shown earlier in (15).

For any other non-zero form of $g(r)$, the total scattering consists of both the specular and the off-specular or diffuse components; For isotropic self-affine rough surfaces without cutoff, the scattering cannot be separated into specular and diffuse components, hence total intensity has to be calculated. The expression for scattering cross-section in (33) can then be simplified using a change of variables from rectilinear to polar coordinates. Using the substitutions $X = r\cos\alpha$ and $Y = r\sin\alpha$ we can write $\mathrm{d}X\mathrm{d}Y = r\mathrm{d}r\mathrm{d}\alpha$. Equation (33) can then be written as

$$\frac{\mathrm{d}\sigma}{\mathrm{d}\Omega} = \frac{\rho^2 r_0^2}{q_z^2} A \int_{-\infty}^{\infty} \mathrm{d}X\mathrm{d}Y e^{-q_z^2 g(X,Y)/2} e^{-i(q_x X + q_y Y)}$$

$$= \frac{\rho^2 r_0^2}{q_z^2} A \int_0^{2\pi} \mathrm{d}\alpha e^{[-i(q_x r\cos\alpha + q_y r\sin\alpha)]} \int_0^{\infty} \mathrm{d}r r e^{-\frac{1}{2}q_z^2 g(r)}. \quad (39)$$

Using the definition

$$J_0(x) = \frac{1}{2\pi} \int_0^{2\pi} e^{ix\sin\alpha} \mathrm{d}\alpha\,, \quad (40)$$

the above equation can be written as

$$\frac{\mathrm{d}\sigma}{\mathrm{d}\Omega} = \frac{2\pi\rho^2 r_0^2}{q_z^2} A \int_0^{\infty} \mathrm{d}r r e^{-(1/2)q_z^2 g(r)} J_0(q_r r)\,, \quad (41)$$

where $q_r = \sqrt{q_x^2 + q_y^2}$. The total scattering intensity can then be written as

$$I = I_0 \frac{2\pi\rho^2 r_0^2}{q_z^2 \sin\alpha_i} \int_0^{\infty} \mathrm{d}r r e^{-(1/2)q_z^2 g(r)} J_0(q_r r) \otimes \mathcal{R}(q_x, q_y, q_z)\,. \quad (42)$$

Here, $\mathcal{R}(q_x, q_y, q_z)$ is the instrumental resolution function. This function takes into account the wave vector resolution of the set up used for measurements and has contributions from the angular and wavelength resolution. In most cases, however, diffuse scattering, which arises due to correlation of heights as a function of lateral displacement, is weak compared to the specular component and it is possible to separate out the two. The correlation function in such cases takes the form as given in (29) and hence, using this form of $g(r)$, (33) can be written as

$$\frac{\mathrm{d}\sigma}{\mathrm{d}\Omega} = \frac{\rho^2 r_0^2}{q_z^2} A e^{-q_z^2\sigma^2} \int_{-\infty}^{\infty} \mathrm{d}X \mathrm{d}Y e^{q_z^2 C(X,Y)} e^{-i(q_x X + q_y Y)}. \tag{43}$$

The above equation can be split into two parts: specular and diffuse. The specular component yields the specular reflectivity following (38) as

$$R = \frac{16\pi^2 \rho^2 r_0^2}{q_z^4} e^{-q_z^2\sigma^2}. \tag{44}$$

The diffuse intensity, I_d, can be written as

$$I_d = I_0 \frac{\rho^2 r_0^2}{q_z^2 \mathrm{sin}\alpha_i} e^{-q_z^2\sigma^2} \int\int \mathrm{d}X \mathrm{d}Y (e^{q_z^2 C(X,Y)} - 1) \\ e^{-i(q_x X + q_y Y)} \otimes \mathcal{R}(q_x, q_y, q_z). \tag{45}$$

In most experiments, the out-of-plane (q_y) resolution is kept coarse to effectively integrate out this component of scattering (refer *Figure* 2). In that situation, the observed intensity can be written as

$$I_d = I_0 \frac{\rho^2 r_0^2}{q_z^2 \mathrm{sin}\alpha_i} e^{-q_z^2\sigma^2} \int\int \mathrm{d}X \mathrm{d}Y (e^{q_z^2 C(X,Y)} - 1) e^{-iq_x X} \\ \int \mathrm{d}q_y e^{iq_y Y} \otimes \mathcal{R}(q_x, q_z) \tag{46}$$

$$= I_0 \frac{\rho^2 r_0^2}{q_z^2 \mathrm{sin}\alpha_i} e^{-q_z^2\sigma^2} \int\int \mathrm{d}X (e^{q_z^2 C(X,0)} - 1) e^{-iq_x X} \otimes \mathcal{R}(q_x, q_y). \tag{47}$$

3. Grazing Incidence SAXS

Grazing incidence small angle X-ray scattering provides information about both lateral and normal ordering at a surface or inside a thin film. This technique combines features from SAXS as well as specular and diffuse X-ray reflectivity. Here, X-rays are incident on the sample at very small grazing angles to the surface and below the critical angle, α_c. As explained earlier, this provides the surface sensitivity due to the TER of X-rays below α_c. In order to make X-ray scattering surface sensitive, typically a grazing incidence angle is kept either below or above the critical angle of the material of the film but always below that of a substrate. When the incident angle is below the critical angle of the film the measurement is sensitive to surface lateral density heterogeneities and when it is above the critical angle of the film it is sensitive to density fluctuations at buried interfaces of the film. The actual choice depends on the system to be studied. In the scattering plane, the GISAXS intensity distribution corresponds to a detector scan in diffuse scattering. For rough surfaces, which contain inhomogeneities in $\rho(z)$ in a direction parallel to the surface, the scattering in non-specular direction is not zero, and one gets what is known as *off-specular* or *diffuse* scattering. The scattering vector $\mathbf{q}$ in such a diffuse scattering measurement contains finite q_x and q_y components. The result then gives information about the surface topology or $\rho(z)$ in the x or y direction. The different components of the scattering vectors are given by

$$q_x = k_0 \cos\alpha_f \cos 2\theta_f - \cos\alpha_i, \tag{48}$$

$$q_y = k_0 \cos 2\theta_f \sin\alpha_f, \tag{49}$$

$$q_z = k_0 \sin\alpha_i + \sin 2\theta_f, \tag{50}$$

where the angles are as defined in *Figure* 4 and $k_{in} = k_0 = (\frac{2\pi}{\lambda})$, λ being the wavelength of incident X-rays.

The scattering intensity $I(q)$ for a lateral electron density fluctuation on the surface can be described as

$$I(q) = \langle F^2 \rangle S(q) \tag{51}$$

where F is the form factor and $S(q)$ is the structure factor. The structure factor describes the spatial arrangement of the objects on the surface and thus their lateral correlations. It is the Fourier transform of autocorrelation function of the object positions. In the simple Born approximation, F is the Fourier transform of the shape function of the objects and is defined as

$$F(\bar{q}) = \int_V \exp(i\bar{q}.\bar{r}) \mathrm{d}^3 r. \tag{52}$$

An example of the contribution from the form factor and the structure factor is shown in *Figure* 4b and c. The full GISAXS intensity map can be theoretically described within the framework of the Distorted-Wave Born-Approximation. GISAXS allows us to record *in situ*, the scattering pattern, as a continuous function of surface concentration to observe any morphological transitions.

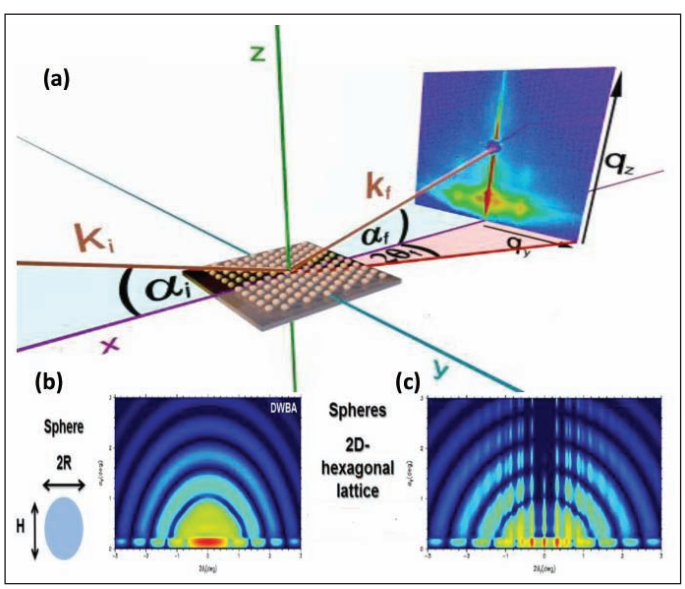

Figure 4. (a) Schematic illustration of the GISAXS set up. (b) The intensity due to spherical form factor and (c) hexagonal arranged spheres. (Adapted from [6])

4. Grazing Incidence Diffraction

In typical GID experiments the evanescent wave is diffracted by lateral two-dimensional order in the monolayer. If the order is crystalline the evanescent wave may be Bragg scattered from a grain which is oriented such that its h, k lattice 'planes' make an angle θ_{hk} with the evanescent beam fulfilling the Bragg condition $\lambda = 2d_{hkl}\sin\theta_{hk}$. There is no restriction on the z-component of the Bragg scattered beam – the Bragg scattered ray may go deeper into the liquid or it may go out of the liquid at an exit angle $\alpha_f > 1$. This is the fundamental difference between the nature of the reciprocal space structure of 2D and conventional 3D crystals. Consider now the variation of intensity with exit angle α_f near α_c. The Bragg scattered ray with $\alpha_f = -\alpha_c$ will be totally reflected by the interface and will interfere constructively with the Bragg scattered ray with $\alpha_f = +\alpha_c$. The exit beam will therefore have a maximum at $\alpha_f = +\alpha_c$.

Figure 5 shows the geometry for in-plane diffraction. The grazing incidence beam illuminates a certain footprint of the surface (as shown at the botton of *Figure* 5). A Soller collimator can transmit X-ray photons from

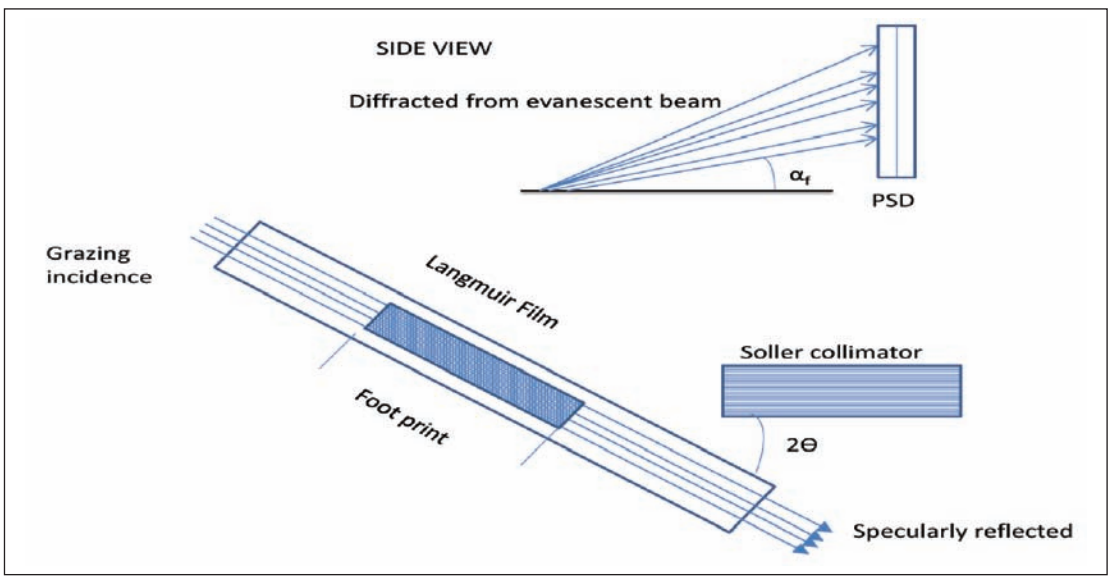

Figure 5. Schematic of GID geometry.
(Adapted from [2].)

part of this footprint if they are diffracted a lateral angle of 2θ and within a fan of vertical angles α_f from the horizon and up to a practical upper limit of around 10°. The vertical angle α_f is determined by a position sensitive detector (PSD) aligned vertically. In this geometry one thus determines the lateral (q_{xy}) as well as the vertical (q_z) components of the scattering vector. Assume now that the sample has 2D (quasi) long range order. This implies that for appreciable scattering to take place q_{xy} must coincide with a reciprocal lattice vector q_{hk} with integer coordinates (h, k) and length $(4\pi/\lambda)\sin\theta_{hk}$. Since most 2D monolayers are found to be composed of randomly oriented 2D crystallites, these systems are essentially a 2D *powder*. Hence, there will always be a crystallite grain with reciprocal lattice vector q_{hk} coinciding with q_{xy} in the crossed beam area of the footprint. There is no selection rule on q_z but the intensity along the (h, k) Bragg rod is modulated with the square of the molecular form factor, cf. right part of *Figure* 6. The form factor of a rod or of a cigar shaped molecule is a disc perpendicular to the molecular axis. Assume first that the rod-like molecules are perpendicular to the surface. The intensity along any Bragg rod will then have its maximum at the horizon. Next, assume that the

Figure 6. The left part of the figure shows the general scattering geometry. k_i and k_f are the wave vectors of the incident and diffracted beams respectively. The scattering vector $q = k_f - k_i$ has components $|q_{xy}| \cong 2k \sin\theta$ parallel to the monolayer plane and $q_z = k \sin \alpha_f$ perpendicular to it. Diffraction takes place when q coincides with a reciprocal lattice point, (1,0,3) in this particular case. The right figure shows that in reciprocal space, the scattering from a 2D crystal extends in rods (Bragg Rods) in the q_z direction, perpendicular to the plane of the monolayer and to its reciprocal 2D net. The scattering vector q must end on an (h, k) Bragg Rod for Bragg diffraction.
(Adapted from [2]).

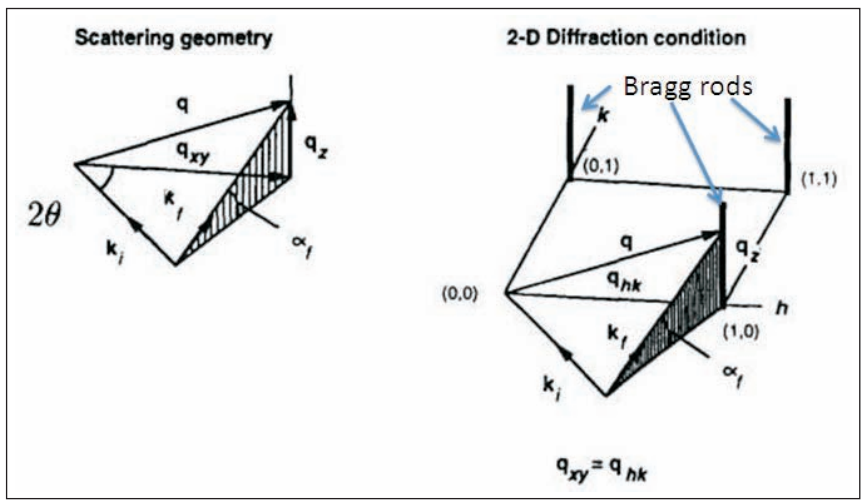

molecules are tilted around a horizontal axis. In a specific example illustrating the point, let us assume that the unit cell is rectangular and that the molecular rotation axis is along $(0, k)$.

In that case, the intercept between the molecular form factor disc and Bragg rod will still have its maximum at the horizon for $(0, k)$ reflections, but for the (h, k) reflections $(h \neq 0)$ the maximum occurs at the intercept of the tilted disc and the (h, k) Bragg rod. We conclude from this example that gives us the intensity distribution along Bragg rods both the tilt angle and the tilt direction of the molecules.

Suggested Reading

[1] **V A Raghunathan, Small Angle X-ray Scattering: Going Beyond the Bragg Peaks, *Resonance*, Vol.85, pp.24–34, 2005.**

[2] **Jens Als-Nielsen, Didier Jacquemain , Kristian Kjaer, Franck Leveiller, Meir Lahav,Leslie Leiserowitz, Principles and applications of grazing incidence x-ray and neutron scattering from ordered molecular monolayers at the air-water interface, *Physics Reports*, Vol.246, pp.251–313, 1994.**

[3] **Jean Daillant and Alain Gibaud, *X-Ray and Neutron Reflectivity: Principles and Applications*, Springer, 1999.**

[4] **Jens Als-Nielsen, Des McMorro, *Elements of Modern X-ray Physics*, John Wiley & Sons, 2011.**

[5] **J K Basu, and Milan K Sanyal, Ordering and growth of Langmuir--Blodgett films: X-ray scattering studies, *Physics Reports*, Vol.363, pp.1–84, 2002.**

[6] **www.gisaxs.de**

Address for Correspondence
Jaydeep K Basu
Physics Department
Indian Institute of Science
Bangalore 560 012, India.
Email:
basu@physics.iisc.ernet.in